

Extreme Cold Events in North America and Eurasia in November–December 2022: A Potential Vorticity Gradient Perspective

Yao YAO^{1,2}, Wenqin ZHUO³, Zhaohui GONG², Binhe LUO⁴, Dehai LUO^{1,2}, Fei ZHENG⁵, Linhao ZHONG⁶, Fei HUANG³, Shuangmei MA⁷, Congwen ZHU⁷, and Tianjun ZHOU⁸

¹CAS Key Laboratory of Regional Climate-Environment for Temperate East Asia, Institute of Atmospheric Physics, Chinese Academy of Sciences, Beijing 100029, China

²University of Chinese Academy of Sciences, Beijing 100049, China

³Frontier Science Center for Deep Ocean Multispheres and Earth System (FDOMES) and Physical Oceanography Laboratory, Ocean University of China, Qingdao 266100, China

⁴State Key Laboratory of Earth Surface Processes and Resource Ecology, Beijing Normal University, Beijing 100875, China

⁵International Center for Climate and Environment Science (ICCES), Institute of Atmospheric Physics, Chinese Academy of Sciences, Beijing 100029, China

⁶National Institute of Natural Hazards, Ministry of Emergency Management of China, Beijing 100085, China

⁷State Key Laboratory of Severe Weather, Chinese Academy of Meteorological Sciences, China Meteorological Administration, Beijing 100081, China

⁸State Key Laboratory of Numerical Modelling for Atmospheric Sciences and Geophysical Fluid Dynamics (LASG), Institute of Atmospheric Physics, Chinese Academy of Sciences, Beijing 100029, China

(Received 20 December 2022; revised 14 January 2023; accepted 28 January 2023)

ABSTRACT

From 17 November to 27 December 2022, extremely cold snowstorms frequently swept across North America and Eurasia. Diagnostic analysis reveals that these extreme cold events were closely related to the establishment of blocking circulations. Alaska Blocking (AB) and subsequent Ural Blocking (UB) episodes are linked to the phase transition of the North Atlantic Oscillation (NAO) and represent the main atmospheric regimes in the Northern Hemisphere. The downstream dispersion and propagation of Rossby wave packets from Alaska to East Asia provide a large-scale connection between AB and UB episodes. Based on the nonlinear multi-scale interaction (NMI) model, we found that the meridional potential vorticity gradient (PV_y) in November and December of 2022 was anomalously weak in the mid-high latitudes from North America to Eurasia and provided a favorable background for the prolonged maintenance of UB and AB events and the generation of associated severe extreme snowstorms. However, the difference in the UB in terms of its persistence, location, and strength between November and December is related to the positive (negative) NAO in November (December). During the La Niña winter of 2022, the UB and AB events are related to the downward propagation of stratospheric anomalies, in addition to contributions by La Niña and low Arctic sea ice concentrations as they pertain to reducing PV_y in mid-latitudes.

Key words: successive cold extremes, atmospheric blocking, NAO, potential vorticity gradient, water vapor backward tracking, Arctic sea ice, La Niña

Citation: Yao, Y., and Coauthors, 2023: Extreme cold events in North America and Eurasia in November–December 2022: A potential vorticity gradient perspective. *Adv. Atmos. Sci.*, **40**(6), 953–962, <https://doi.org/10.1007/s00376-023-2384-3>.

* Corresponding author: Yao YAO
Email: yaoyao@tea.ac.cn

1. Introduction

From 17 November to 27 December 2022, North America, Europe, and East Asia were hit by successive extreme cold snowstorms. From 17–19 November, North America was hit by an extreme cold wave, with snowstorms hitting parts of New York State (<https://edition.cnn.com/2022/11/20/weather/buffalo-new-york-great-lakes-snowstorm-sunday/index.html>). From 26 November into early December, China experienced a strong nationwide cold wave. An extremely low temperature of -48.6°C was observed in Altay, Xinjiang, where heavy snowstorms and extreme cold contributed to the deaths of local residents (<http://www.inewsweek.cn/society/2022-12-05/17185.shtml>). In mid-December, North America and East Asia were again hit by extreme cold events. Then, around 25 December, North America experienced a “bomb cyclone”, which led to the coldest Christmas in nearly 40 years and caused huge social and economic damage (<https://globalnews.ca/news/9372586/us-storm-power-outages-christmas-plans/>).

The frequent extreme cold weather that occurred in November and December has become a matter of great concern to both the public and the research community. Recent studies indicate that although Eurasia tends to experience more frequent cold air outbreaks and heavy snowfall during La Niña winters, a skillful seasonal forecast needs to combine information regarding the North Atlantic Oscillation (NAO), the anomalous anticyclone near the Ural Mountains, and the tendency for the occurrence of cold air invasions triggered by the synergistic effect of a warm Arctic and a cold tropical Pacific on the hemispheric scale (Luo et al., 2021; Zheng et al., 2022c). Extreme cold events in mid-latitudes in winter are a direct effect and manifestation of the weakening, collapse, and re-establishment of the westerly jet (Yao et al., 2017), which is a major weather process in winter and exerts an important impact on human health and social activities (Mu et al., 2022). The prediction of extreme cold weather at subseasonal to seasonal time scales is a great challenge due to its strong dynamic nonlinear characteristics and uncertainties (Bueh et al., 2022; Dai et al., 2022; Zhang et al., 2022b; Zheng et al., 2022a). Specific atmospheric circulation modes that cause extreme cold weather include local blocking (Bueh et al., 2022; Yao et al., 2022), the NAO (Iles and Hegerl, 2017; Li et al., 2022), and the Arctic Oscillation (Chen et al., 2013; Cohen et al., 2010; Park et al., 2011). These modes can excite significant meridional circulation anomalies, further promoting and guiding the southward movement of cold Arctic air, which affects lower latitudes.

The impact of global warming on extreme cold events has received widespread attention (Luo et al., 2021; Yao et al., 2022; Zheng et al., 2022b). While it is indisputable that global warming leads to a decrease in cold extremes in long-term climate projections, forecasting such cold extremes remains a challenge for short-term climate prediction. Some studies have also revealed the relationship between a warm Arctic and a cold continent and its influence on extreme weather from the perspective of meridional potential vorticity gradient (PV_y) based on a nonlinear multi-scale interaction model (Luo et al., 2019a; 2019b), which is an important indicator to reveal the occurrence of extreme cold weather. In the winter of 2020/21, extreme cold events from East Asia to North America have been widely studied (Mu et al., 2022; Zhang et al., 2022b). The physical processes and mechanisms of this extreme cold event in China have been described from a synergistic perspective (Yao et al., 2022; Zhang et al., 2022a; Zhang et al., 2022c; Zheng et al., 2022b). The predictability of three extreme cold events in East Asia has been described by Dai et al. (2022). The strong cold surge sweeping through eastern and northwestern China during 4–9 November 2021 has also been a focus of the climate research community (Zhou et al., 2022). Some studies have analyzed cold extremes from the perspective of circulation anomalies (Li et al., 2022; Li et al., 2019; Luo et al., 2016a; 2016b; Ma and Zhu, 2021; Yu et al., 2022a) and isentropic mass circulation (Yu et al., 2022b). In addition, Ma and Zhu (2023) discussed the physical process of the sharp subseasonal swing of intercontinental cold and warm extremes over North America and Eurasia. They found the North-Pacific-Oscillation-like phase transition regulated by the unprecedented SST warming in the North Atlantic to be the main process. Whether the existing mechanisms help to explain the cold extremes in the later months of 2022 remains unknown, and its elucidation is a motivating factor behind the study.

This study aims to reveal the physical mechanisms associated with the frequent occurrence of extreme cold events in November–December from the perspective of PV_y . The following issues are addressed: 1) What atmospheric circulation regimes accompanied these extreme cold events and what were the possible connections between them? 2) What was the physical background of these frequent extreme cold events? 3) What were the characteristics of the water moisture source pathways of the two key snowstorm processes?

2. Data and Methodology

2.1. Datasets

The datasets used in this study are from the latest reanalysis dataset (Hersbach and Dee, 2016) from the European Centre for Medium-Range Weather Forecasts (ERA5), including the multi-level geopotential height, horizontal wind components (u and v), surface air temperature (SAT), and snowfall, all at a $1^{\circ} \times 1^{\circ}$ spatial resolution from 1979 to 2022. In addition, the high resolution ($0.25^{\circ} \times 0.25^{\circ}$) daily mean ERA5 variables, including precipitable water, vertically integrated water vapor, and vertically integrated eastward and northward water vapor transport, were derived from backward trajectory analysis

(Zhong et al., 2018). We used a modified NAO index (Li and Wang, 2003) to identify NAO cases with position-shifted mean states. Here, the NAO index in November and December 2022 is defined as the difference in the normalized daily sea level pressure averaged over the North Atlantic sector (80°W–30°E) between 30°N and 60°N. The monthly Arctic sea ice concentration (SIC) dataset was obtained from the National Snow and Ice Data Center.

2.2. Methods

As revealed from the nonlinear multi-scale interaction (NMI) model (Luo et al., 2019a; 2019b) of atmospheric blocking, the meridional gradient of the background potential vorticity (PV_y) is a key physical indicator for the maintenance of atmospheric blocking. The non-dimensional form of PV_y in the equivalent barotropic atmosphere is expressed as $PV_y = \partial PV / \partial y = \beta - \partial^2 U / \partial y^2 + FU$ (Luo et al., 2019a), where U is the non-dimensional zonal wind, β is the non-dimensional meridional gradient of the Coriolis parameter at a given reference latitude, and $F = (L/R_d)^2$, where L is the characteristic length (~1000 km) and $R_d \sim 1000$ km is the Rossby radius deformation. When PV_y is small, atmospheric blocking is characterized by weak energy dispersion and strong nonlinearity, allowing it to maintain itself for a long time. Thus, a small PV_y is favorable for maintaining atmospheric blocking (Luo et al., 2019a). A Hovmöller diagram (Hovmöller, 1948) is used to show the propagation of Rossby wave packets. A spatially unbounded dynamical recycling model, developed by Dominguez et al. (2006) and further extended by Zhong et al. (2018), was applied here to quantitatively examine backward moisture trajectories and water vapor contributions in target regions. For details regarding the calculation methods and model descriptions, please refer to Zhong et al. (2018). In our analysis, the daily (monthly) anomalies are defined as the deviation of the daily (monthly) field from its climatological time mean of 1979–2020.

3. Extreme cold events in November and December 2022 and their physical background

3.1. Time evolution of circulation regimes

Figure 1 shows the time-mean of the 500-hPa geopotential height field and SAT anomalies for the four major extreme cold events. A blocking high formed over Alaska and peaked during 17–19 November (Fig. 1a), and the downstream low-

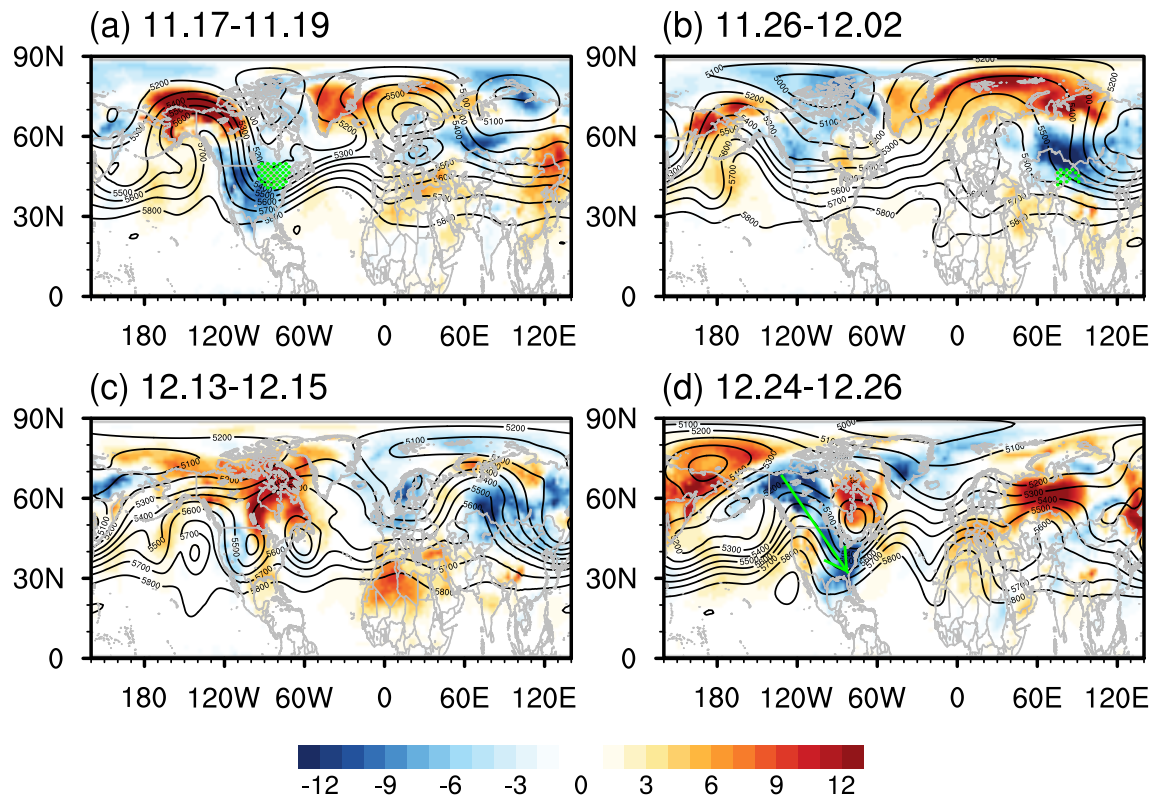


Fig. 1. Time-mean surface air temperature anomaly (shading, units: K) and 500-hPa geopotential height (contour, units: gpm, contour interval = 100 gpm) for the four stages: (a) 17–19 November, (b) 26 November – 2 December, (c) 13–15 December, and (d) 24–26 December that were associated with the several extreme cold events. Key snowfall areas in (a) and (b) are marked with green dots. All the anomalies are calculated relative to the mean conditions of 1979–2020.

pressure trough deepened significantly. Over the North Atlantic region, the observed pattern corresponded to a positive NAO (NAO+) structure associated with a strong zonal jet. Such a circulation regime is conducive to the polar vortex penetrating toward lower latitudes, leading to a widespread cooling process. Significant negative SAT anomalies are seen over North America, while warm anomalies were witnessed in Alaska, the Bering Strait, and parts of the adjacent Arctic Ocean. In addition, northwest New York State and the five Great Lakes, located in the center of the low-pressure trough, received significant snowfall (green dotted region) between 17–19 November, resulting in severe blizzard conditions.

One week after the North American blizzard ended, from November 26 to early December, this winter's first extreme cold wave swept through continental China, causing widespread cooling and snowfall across the country. [Figure 1b](#) illustrates the dominant circulation regime for this event, consisting of a large blocking high that appeared over Eurasia from 26 November to 2 December. The blocking further strengthened and moved eastward, translating into a Ural Blocking (UB) event, causing a trough of low pressure to further deepen downstream ([Fig. S1](#) in the Electronic Supplementary Material, ESM). The strong push of cold air first affected Northwest China as the leading edge of the low-pressure trough reached the Xinjiang region on November 26 and caused record-breaking low temperatures and heavy snowfall in this area. Then, after November 27, the UB high continued to develop and shift to the southeast, allowing the trough of low pressure to move further to the east and south, affecting the central and southern parts of China. From November 26 to 29, the western Pacific subtropical high lifted northward and extended westward ([Fig. S1](#) in the ESM, bold black 5880 gpm line), which was closely related to the northward movement of the southern rain band in China from November 26 to 29 (figure not shown).

In mid-December, North America and East Asia were simultaneously hit by another extreme cold process. [Figure 1c](#) shows that the circulation regime in North America exhibited a hybrid pattern. The Alaska blocking (AB) ridge is displaced significantly to the south, and the downstream low pressure caused cooling in some parts of North America. In addition, another ridge is found in the North Atlantic region, which corresponds to a negative NAO (NAO-) pattern. The low-pressure center corresponding to the NAO- was close to the eastern part of the North American continent, allowing for the two low-pressure centers to combine. This interaction led to a cooling process and a cyclonic circulation in North America that was accompanied by a tornadic outbreak. At the same time, East Asia was dominated by a lower-latitude UB ridge, which triggered a widespread cooling process.

During the subsequent Christmas season, North America was again hit by an extreme cold weather process. The associated “bomb cyclone” affected nearly the entirety of the North American continent, including Canada and the United States, causing record-breaking low temperatures and snowfall. [Figure 1d](#) shows that North America was controlled by a lower latitude AB ridge around 120°W, while a strong North Pacific blocking was present at higher latitudes to the northwest. This pattern represents a complex circulation regime where one high ridge is nested within another stronger blocking high. The two nested blocking ridges allow for a “relay effect” (as shown by the green arrow) to occur within their downstream low-pressure centers as well, allowing a large amount of cold air from the polar regions to reach the North American continent directly. Moreover, it is noted that the SAT anomalies show a west-east seesaw on synoptic-scale timescales between North America and Eurasia ([Fig. 1](#)), even though the cold events are frequent.

These major extreme cold processes have a commonality in that they are closely related to local blocking and NAO regimes, but their local details vary. Next, we employ a larger-scale view to reveal the physical processes and background linkages of these extreme cold events.

3.2. A connection between local circulation regimes

[Figure 2a](#) shows a Hovmöller diagram of daily 500-hPa geopotential height anomalies averaged over 40°–70°N from 12 November to 27 December 2022, corresponding to the propagation of a Rossby wave packet. It can be seen that there are significant and frequent propagation processes of the Rossby wave packet (shown by black arrows) from the North Pacific to the Eurasian region during the period from mid-November to the end of December. AB events were frequently generated during this period (AB1 to AB4), and the NAO shifted from a positive phase in November to a negative phase in December (the index is shown in [Fig. 2b](#)). The UB in Eurasia also shows significant activity, but is dependent on the phase of the NAO. The Rossby wave train associated with NAO+ in November is favorable for the production and maintenance of the UB ([Luo et al., 2018; Luo et al., 2016b](#)), because it exhibits a wavenumber two structure with a positive anomaly over Eurasia. In December, after the NAO transitioned to a negative phase, the Rossby wave train evolved into a wavenumber three structure, which is not conducive to the generation and maintenance of a UB, because a negative anomaly appears downstream of the North Atlantic. Therefore, UB activity decreased significantly in December. Although the frequent extreme cold events in November–December were attributed to local blocking and NAO processes, the frequent activity of these regimes is linked to the activity of the Rossby wave train, thus demonstrating their remote connection.

[Figure 2b](#) shows the temporal variations of the AB and UB intensities in addition to the NAO index. The UB and AB indexes are constructed based on the grid point where the maximum value of the respective daily blocking anticyclonic center is located, and a regional average is calculated over a 20° latitude × 60° longitude box centered on that grid point. It is found that the AB precedes the NAO+, whereas the intensification of the UB lags the decay of NAO+. In contrast, the suppressed UB activity in December is related to the presence of NAO-. Thus, the generation and persistent intensification of a

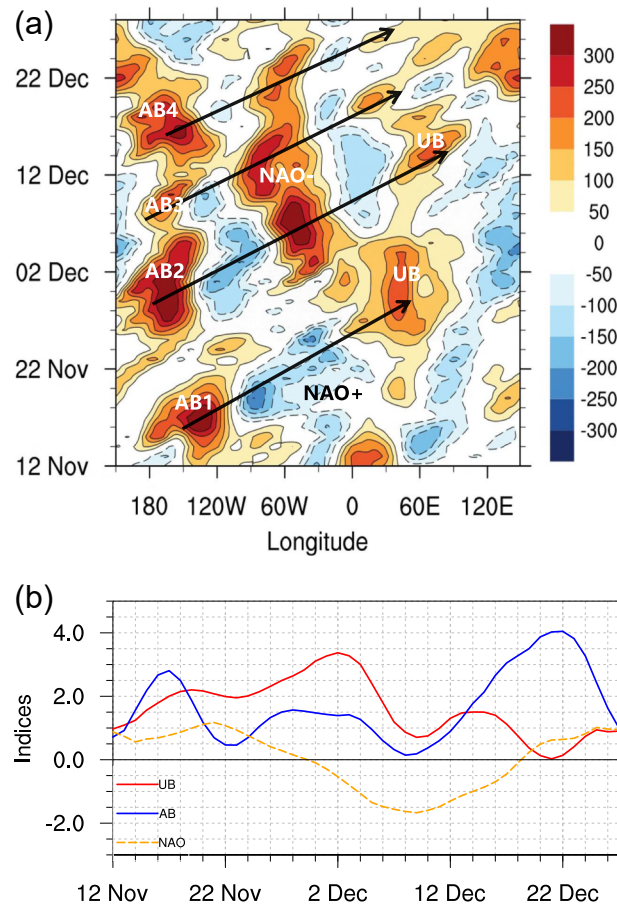


Fig. 2. (a) Hovmöller diagram of the daily 500-hPa geopotential height anomalies (shading and contour, units: gpm) averaged over 40°–70°N from 12 November to 27 December 2022. AB1 to AB4 represent four Alaska blocking events. Black lines with arrows indicate the propagation of Rossby wave packets. All the anomalies are calculated relative to the mean condition of 1979–2020. (b) Daily normalized indices of UB, AB, and NAO from 12 November to 27 December. The UB and AB indexes are based on dynamic tracking and regional averaging of the corresponding blocking anticyclonic centers.

UB in November is connected to the AB through the change of the NAO index from a positive to a negative value, as revealed by Luo et al. (2016b, 2018), from the energy dispersion perspective of a Rossby wave train.

In addition, we examined the signal throughout the troposphere and stratosphere. Figure 3 shows the regional mean geopotential height anomalies as a function of vertical levels from 6 November to 27 December. Figure 3a shows that in the Eurasian region, there is a downward-propagating stratospheric anomaly signal to the troposphere, as indicated by the black arrow. This process corresponded to the extreme snowstorm process in East Asia in late November and early December. A significant downward-propagating stratospheric signal in the North Pacific can also be observed from the middle through the end of December. The strong anticyclonic center in the troposphere is the blocking process that caused the “bomb cyclone” in North America. The downstream propagation of wave activity and the propagation between the stratosphere and troposphere can also be seen from the diagnosis of wave flux (Takaya and Nakamura, 2001), which is neither shown nor analyzed due to space limitation. In summary, frequent local blocking, Rossby wave packet propagation, NAO phase transition, and downward propagating stratospheric anomalies synergistically contribute to frequent extreme cold events during November–December.

The mean life span of a blocking event is about 5–8 days (Tibaldi and Molteni, 1990; Yao et al., 2017). However, in this November event, the UB lasted more than 20 days, while the AB lasted for nearly 20 days during December. Although

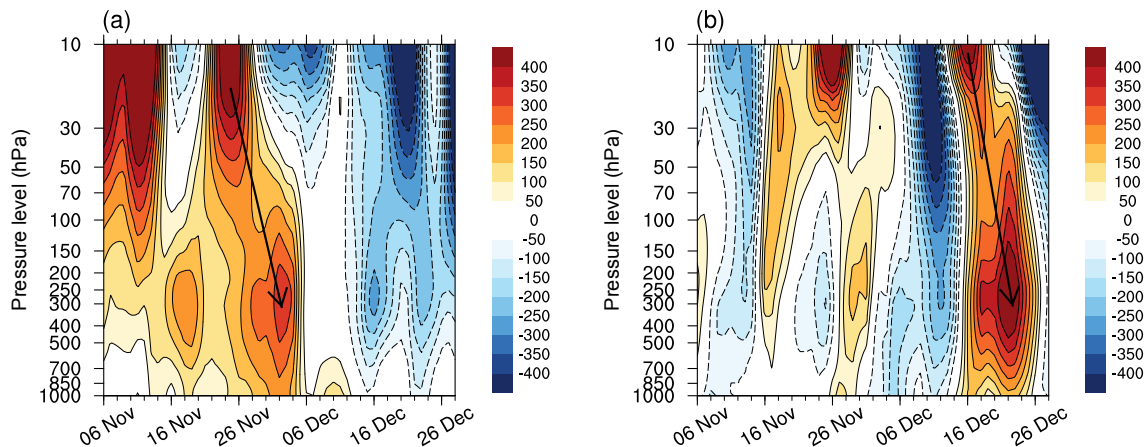


Fig. 3. The regionally averaged geopotential height anomalies (shading and contour, units: gpm) for (a) 0° – 60° E, 60° – 80° N and (b) 140° E– 160° W, 60° – 80° N as a function of vertical levels from 6 November to 27 December. Black lines with arrows indicate the downward propagation of a stratospheric anomaly signal. All the anomalies are calculated relative to the mean condition of 1979–2020.

the generation of a UB results from the dispersion and propagation of upstream wave trains associated with AB and NAO+ events, the persistent maintenance of a UB may be related to favorable background conditions.

3.3. Physical background of extreme cold events from a PV_y perspective

Figure 4a shows the time mean distribution of the PV_y anomalies from November to December 2022. Notably, PV_y exhibits significant negative anomalies in mid-high latitudes from North America to Eurasia (Fig. 4a). Thus, the weak PV_y in mid-latitudes is conducive to maintaining AB and UB events (Luo et al., 2019a). This explains why the AB and UB events lasted for about 20 days. Figure 4b further shows the variation of zonal mean PV_y as a function of latitude for November–December in 2022. The averaged PV_y for November to December 2022 (black line) is extremely low, with most mid-high latitudes (52° – 70° N) below the lower quartile values from 1979–2022. In addition, the difference in composite PV_y between La Niña and El Niño years is shown in Fig. 4c. It was found that La Niña years are favorable for the weakening of PV_y in mid-latitudes (46° to 60° N, above the 90% confidence level around 50° N). The same composite comparison is also applied to low SIC years (below -0.3 std) and high SIC years (above 0.3 std). The differences are mainly concentrated in mid-high latitudes (50° – 70° N), and the PV_y is small in low SIC years compared to high SIC years. This implies that both low SIC and La Niña events favor weak PV_y in the mid-latitudes. However, the effect of low SIC on the reduction of mid-latitude PV_y was not as profound as those of La Niña. The comparison between La Niña years with low SIC and El Niño years with high SIC (red line) shows that their combination (La Niña years with low SIC) benefits weaker PV_y in mid-latitudes (above the 90% confidence level around 50° N). This setting was consistent with the physical background of the frequent extreme cold events in November–December 2022 and with the synergistic effects of La Niña and Arctic SIC from the perspective of PV_y . Notably, our study can also explain why UB events differed in November and December. Although the mid-latitude PV_y anomalies are weak in both November and December and favor UB events, the positive (negative) phase of NAO can promote (inhibit) the formation of a UB (Luo et al., 2016b). Thus, the NAO+ in November is favorable for the generation and maintenance of a downstream UB, but the NAO– in December suppresses the maintenance of UB. Consequently, there is a large difference in UB characteristics between November and December.

3.4. Backward trajectories of water vapor for two key snowstorm processes

Since North America and East Asia both suffered from disastrous snowstorms, it is necessary to analyze the source of water moisture during the two key snowfall processes. Figure 5 shows the distribution of 15-day backward moisture trajectories for the Great Lakes in the United States and Altay in Xinjiang China. The main moisture trajectories to the Great Lakes include the pathways from the Arctic Ocean, the Western Pacific, the Bering Strait, and scattered areas in western North America (Figs. 5a–c). The snowfall process lasted for three days, showing different water moisture pathways each day. On November 17 (Fig. 5a), the contribution ratio (shading) of water moisture trajectories from the Arctic Ocean was the highest, contributing more than 80% and even nearly 100% in some areas. The contribution ratio by the Arctic Ocean on November 18 (Fig. 5b) was still large, but parts of the Northwest Pacific had also made significant contributions. On November 19 (Fig. 5c), the contribution of moisture trajectories came mainly from the Bering strait and surrounding areas. In addition, the distribution of the moisture sources (Figs. S2a, c, and e in the ESM) displays a pattern with more local characteristics. In general, the greatest evaporation contribution comes locally, from the Great Lakes themselves, which have prominent evap-

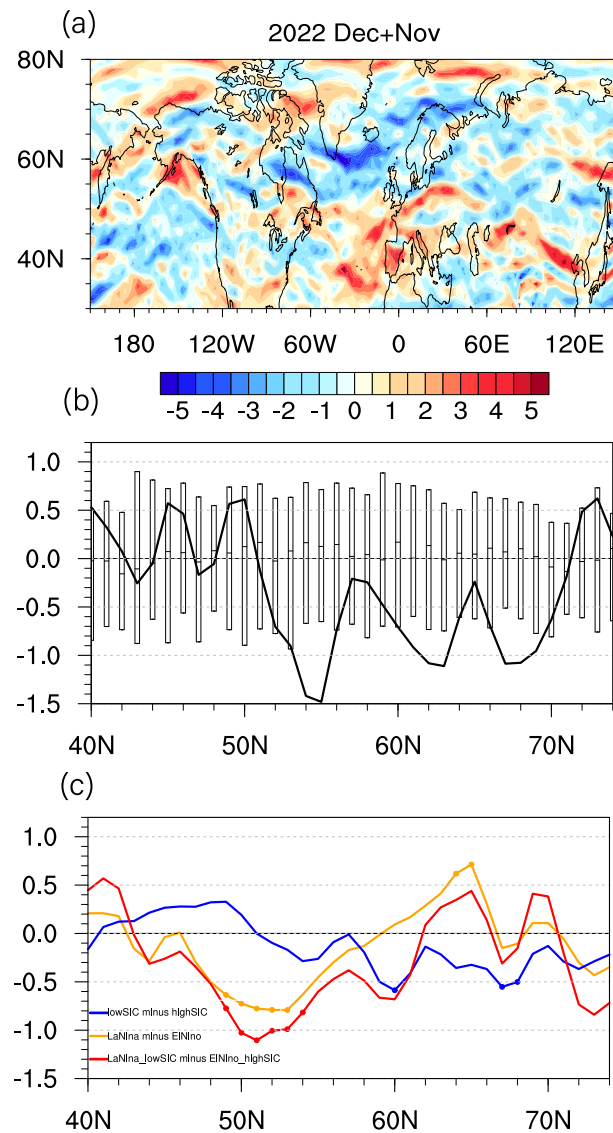


Fig. 4. (a) The monthly mean distribution of the nondimensional PV_y anomalies for November and December 2022 (shading). (b) Zonal mean PV_y anomalies as a function of latitudes for November–December, the black line represents 2022. The box plot indicates the dispersion of upper, median, and lower quartile values for PV_y anomalies from 1979–2022. (c) Composite differences of PV_y anomalies as a function of latitude. The blue line represents low SIC (23) years minus high SIC (21) years, the yellow line represents La Niña (18) years minus El Niño (14) years, and the red line represents La Niña (11) years with low SIC minus El Niño (6) years with high SIC. The dots represent latitudes above the 90% confidence level based on a two-tailed Student’s t-test.

oration sources that are vital for its water vapor supply. The distributions of trajectories (Figs. S2b, d, and f) indicate that the Great Lakes are mainly influenced by the westerlies and their changes associated with an AB, as depicted in Fig. 1a.

Figures 5d–e show the distribution of 15-day backward moisture trajectories for Altay. The main moisture pathways to Altay are from the Arctic Ocean and the North Atlantic, associated with the branch of westerlies caused by Eurasian blocking. The contribution ratio (shading) of the Arctic was larger than the North Atlantic on 25 November, and on 26 November, the contribution ratio of the North Atlantic was even larger. The moisture contribution (Fig. S3a and c in the ESM) indicated that the contribution of water vapor to the snowfall in Altay and its surrounding areas mainly came from external sources.

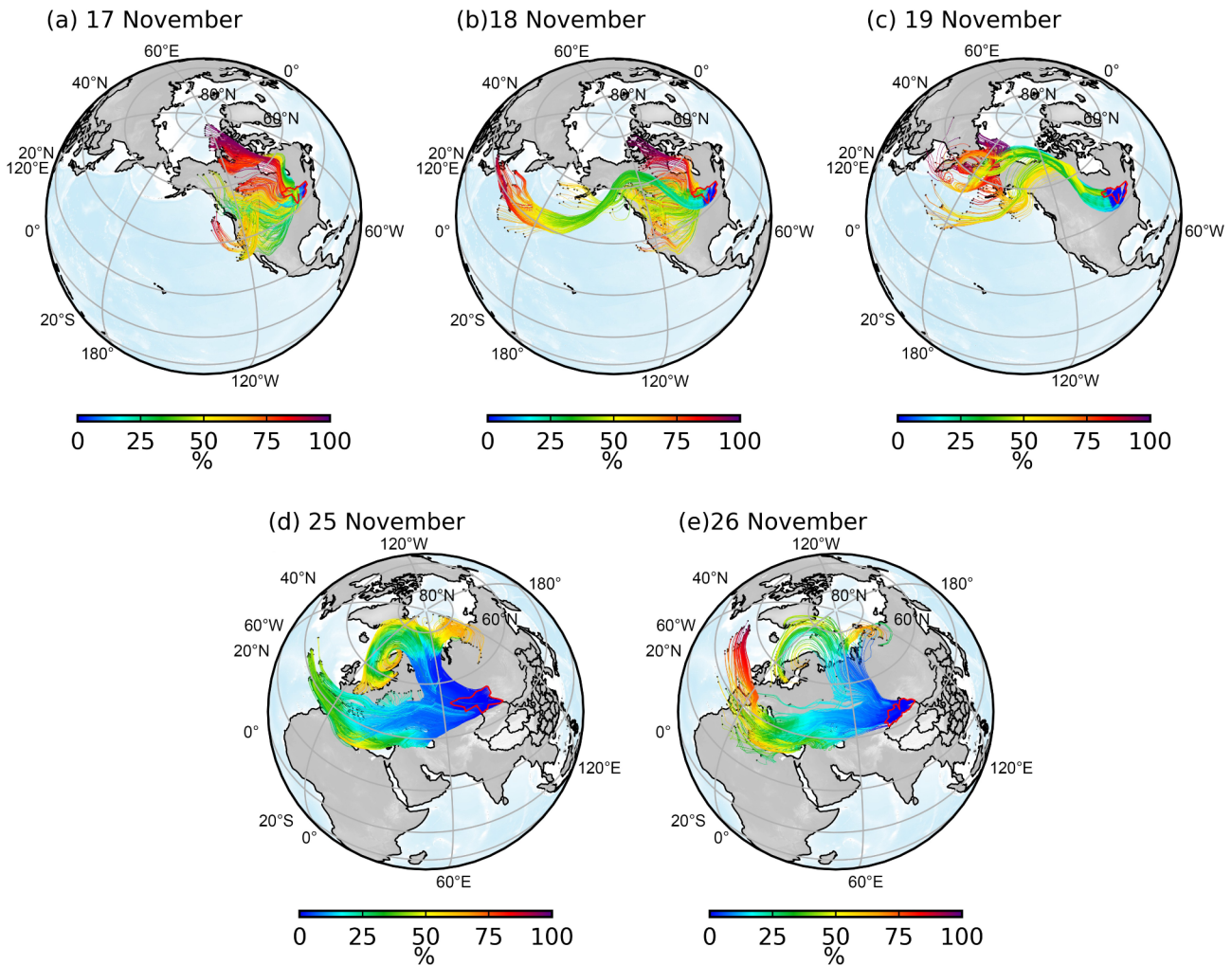


Fig. 5. The 15-day backward moisture trajectories for the Great Lakes on (a) 17 November, (b) 18 November, and (c) 19 November 2022, and for the Altay region on (d) 25 November and (e) 26 November 2022. The color of the trajectory indicates the accumulated moisture contribution ratio (units: %) from a given location on the trajectory to the origin of a backward trajectory (target region). The domains bounded by the red lines are the Great Lakes and the Altay regions.

The trajectory count distributions (Figs. S3b and d) suggest that the moisture pathway is closely associated with the change in the westerly jet caused by the blocking circulation.

4. Summary and discussion

Extreme cold events frequently occurred from North America to Eurasia in November and December 2022. The atmospheric circulation regime corresponding to each event was examined. Snowstorms in North America are associated with frequent AB, while cold extremes in East Asia are closely related to UB. It is found that the circulation regime that dominated the cooling process in East Asia starting on November 26 was a strong, extensive, and long-lived UB, which lasted for more than 20 days. In addition, the North American “bomb cyclone” around 25 December was associated with the combined effects of strong North Pacific blocking and a lower latitude AB ridge. In mid-December, the squeeze of the NAO– and the AB created two low-pressure cyclonic centers over North America, causing cooling and tornadic outbreaks.

Analysis based on a traditional Hovmöller diagram reveals that frequent propagation of Rossby wave packets occurred from the North Pacific to Eurasia in November and December 2022, implying a remote connection between these extreme events. The NAO+ in November contributed to the maintenance and strengthening of the UB, and the positive-to-negative transition of the NAO phase also supported the weakening of UB activity in December. The change in the Rossby wavenumber from two to three associated with the NAO phase transition is the main dynamic difference between November and December. Further, the two downward propagating stratospheric anomaly signals in East Asia and North America provide important energy supplements for the long-lived UB and AB events. The diagnosis of wave activity flux also corroborates these processes (figure not shown).

The PV_y anomalies are negative in mid-high latitudes in November and December 2022, which are favorable conditions for the formation of AB and UB events, as well as for their longevity, even though UB is significantly influenced by upstream wave trains associated with AB events and the NAO phase. Further composites based on long-term climate series imply that both La Niña and low SIC conditions favor the formation of weak PV_y at mid-latitudes. The combination of La Niña and low SIC conditions can further favor the weakening of mid-latitude PV_y , which is an important reason for the frequent extreme cold in November–December 2022. The PV_y based on the NMI model used in this paper provides a unique perspective for understanding the physical processes of extreme cold events. If a small PV_y continues in January–February 2023, it is expected that longer-lived UB events can frequently occur and lead to frequent severe cold extremes in late winter.

In addition, the moisture pathway of the two key snowstorm processes is closely related to the wave guidance and transport of westerlies. For the snowstorm near the Great Lakes, the local water vapor transport of the five Great Lakes plays the most important role. The water moisture pathways of Altay snowstorm came mainly from the North Atlantic and the Arctic Ocean, implying that the moisture source of this snowfall is mainly the contribution of external water vapor, and the contribution of local water vapor is small.

By focusing on the frequent extreme cold events of November to December 2022, we reveal the possible influence of AB and UB events and their connection under the background of La Niña and SIC from the perspective of PV_y . However, many other factors which affect extreme weather and climate need further examination, including those related to observation, modeling results, and theory.

Acknowledgements. The authors acknowledge support from the National Natural Science Foundation of China (Grant Nos. 41975068, 42150204, 42288101, 42075024, and 41830969). We thank Dr. W. Q. ZHANG for constructive discussions regarding the calculations.

Electronic supplementary material: Supplementary material is available in the online version of this article at <https://doi.org/10.1007/s00376-023-2384-3>.

REFERENCES

- Bueh, C., J. B. Peng, D. W. Lin, and B. M. Chen, 2022: On the two successive supercold waves straddling the end of 2020 and the beginning of 2021. *Adv. Atmos. Sci.*, **39**, 591–608, <https://doi.org/10.1007/s00376-021-1107-x>.
- Chen, W., X. Q. Lan, L. Wang, and Y. Ma, 2013: The combined effects of the ENSO and the Arctic Oscillation on the winter climate anomalies in East Asia. *Chinese Science Bulletin*, **58**, 1355–1362, <https://doi.org/10.1007/s11434-012-5654-5>.
- Cohen, J., J. Foster, M. Barlow, K. Saito, and J. Jones, 2010: Winter 2009–2010: A case study of an extreme Arctic Oscillation event. *Geophys. Res. Lett.*, **37**, L17707, <https://doi.org/10.1029/2010GL044256>.
- Dai, G. K., C. X. Li, Z. Han, D. H. Luo, and Y. Yao, 2022: The nature and predictability of the East Asian extreme cold events of 2020/21. *Adv. Atmos. Sci.*, **39**, 566–575, <https://doi.org/10.1007/s00376-021-1057-3>.
- Dominguez, F., P. Kumar, X.-Z. Liang, and M. F. Ting, 2006: Impact of atmospheric moisture storage on precipitation recycling. *J. Climate*, **19**, 1513–1530, <https://doi.org/10.1175/JCLI3691.1>.
- Hersbach, H., and D. Dee, 2016: ERA5 reanalysis is in production. ECMWF Newsletter, No. 147.
- Hovmöller, E., 1948: North-South cross section of temperature, relative humidity, and wind in a well-marked zonal current over western Europe. *J. Meteorol.*, **5**, 67–69, [https://doi.org/10.1175/1520-0469\(1948\)005<0067:NSCSOT>2.0.CO;2](https://doi.org/10.1175/1520-0469(1948)005<0067:NSCSOT>2.0.CO;2).
- Iles, C., and G. Hegerl, 2017: Role of the North Atlantic Oscillation in decadal temperature trends. *Environmental Research Letters*, **12**, 114010, <https://doi.org/10.1088/1748-9326/aa9152>.
- Li, J. P., and J. X. L. Wang, 2003: A new North Atlantic Oscillation index and its variability. *Adv. Atmos. Sci.*, **20**, 661–676, <https://doi.org/10.1007/BF02915394>.
- Li, J. P., T. J. Xie, X. X. Tang, H. Wang, C. Sun, J. Feng, F. Zheng, and R. Q. Ding, 2022: Influence of the NAO on wintertime surface air temperature over East Asia: Multidecadal variability and decadal prediction. *Adv. Atmos. Sci.*, **39**, 625–642, <https://doi.org/10.1007/s00376-021-1075-1>.
- Li, Y., J. Y. Zhang, Y. Lu, J. L. Zhu, and J. Feng, 2019: Characteristics of transient eddy fluxes during blocking highs associated with two cold events in China. *Atmosphere*, **10**, 235, <https://doi.org/10.3390/atmos10050235>.
- Luo, B. H., D. H. Luo, A. G. Dai, I. Simmonds, and L. X. Wu, 2021: A connection of winter Eurasian cold anomaly to the modulation of ural blocking by ENSO. *Geophys. Res. Lett.*, **48**, e2021GL094304, <https://doi.org/10.1029/2021GL094304>.
- Luo, D. H., Y. Q. Xiao, Y. Yao, A. G. Dai, I. Simmonds, and C. L. E. Franzke, 2016a: Impact of ural blocking on winter warm arctic-cold Eurasian anomalies. Part I: Blocking-induced amplification. *J. Climate*, **29**, 3925–3947, <https://doi.org/10.1175/JCLI-D-15-0611.1>.
- Luo, D. H., Y. Q. Xiao, Y. N. Diao, A. G. Dai, C. L. E. Franzke, and I. Simmonds, 2016b: Impact of ural blocking on winter warm arctic-cold Eurasian anomalies. Part II: The link to the North Atlantic oscillation. *J. Climate*, **29**, 3949–3971, <https://doi.org/10.1175/JCLI-D-15-0612.1>.
- Luo, D. H., X. D. Chen, and S. B. Feldstein, 2018: Linear and nonlinear dynamics of North Atlantic oscillations: A new thinking of symmetry breaking. *J. Atmos. Sci.*, **75**, 1955–1977, <https://doi.org/10.1175/JAS-D-17-0274.1>.
- Luo, D. H., W. Q. Zhang, L. H. Zhong, and A. G. Dai, 2019a: A nonlinear theory of atmospheric blocking: A potential vorticity gradient

- view. *J. Atmos. Sci.*, **76**, 2399–2427, <https://doi.org/10.1175/JAS-D-18-0324.1>.
- Luo, D. H., X. D. Chen, J. Overland, I. Simmonds, Y. T. Wu, and P. F. Zhang, 2019b: Weakened potential vorticity barrier linked to recent winter arctic sea ice loss and midlatitude cold extremes. *J. Climate*, **32**, 4235–4261, <https://doi.org/10.1175/JCLI-D-18-0449.1>.
- Ma, S. M., and C. W. Zhu, 2021: Atmospheric circulation regime causing winter temperature whiplash events in North China. *International Journal of Climatology*, **41**, 917–933, <https://doi.org/10.1002/joc.6706>.
- Ma, S. M., and C. W. Zhu, 2023: Subseasonal swing of cold and warm extremes between Eurasia and North America in winter of 2020/21: initiation and physical process. *Environ Res Lett*, **18**, 014023. <https://doi.org/10.1088/1748-9326/acaabf>.
- Mu, M., D. H. Luo, and F. Zheng, 2022: Preface to the special issue on extreme cold events from East Asia to North America in winter 2020/21. *Adv. Atmos. Sci.*, **39**, 543–545, <https://doi.org/10.1007/s00376-021-1004-3>.
- Park, T.-W., C.-H. Ho, and S. Yang, 2011: Relationship between the Arctic Oscillation and Cold Surges over East Asia. *J. Climate*, **24**, 68–83, <https://doi.org/10.1175/2010JCLI3529.1>.
- Takaya, K., and H. Nakamura, 2001: A formulation of a phase-independent wave-activity flux for stationary and migratory quasigeostrophic eddies on a zonally varying basic flow. *J. Atmos. Sci.*, **58**, 608–627, [https://doi.org/10.1175/1520-0469\(2001\)058<0608:AFOAPI>2.0.CO;2](https://doi.org/10.1175/1520-0469(2001)058<0608:AFOAPI>2.0.CO;2).
- Tibaldi, S., and F. Molteni, 1990: On the operational predictability of blocking. *Tellus A*, **42**, 343–365, <https://doi.org/10.1034/j.1600-0870.1990.t01-2-00003.x>.
- Yao, Y., D. H. Luo, A. G. Dai, and I. Simmonds, 2017: Increased quasi stationarity and persistence of winter ural blocking and eurasian extreme cold events in response to arctic warming. Part I: Insights from observational analyses. *J. Climate*, **30**, 3549–3568, <https://doi.org/10.1175/JCLI-D-16-0261.1>.
- Yao, Y., W. Q. Zhang, D. H. Luo, L. H. Zhong, and L. Pei, 2022: Seasonal cumulative effect of ural blocking episodes on the frequent cold events in China during the early winter of 2020/21. *Adv. Atmos. Sci.*, **39**, 609–624, <https://doi.org/10.1007/s00376-021-1100-4>.
- Yu, M. J., S. M. Ma, and C. W. Zhu, 2022a: The alternating change of cold and warm extremes over North Asia during winter 2020/21: Effect of the annual cycle anomaly. *Geophys. Res. Lett.*, **49**, e2021GL097233, <https://doi.org/10.1029/2021GL097233>.
- Yu, Y. Y., Y. F. Li, R. C. Ren, M. Cai, Z. Y. Guan, and W. Huang, 2022b: An isentropic mass circulation view on the extreme cold events in the 2020/21 winter. *Adv. Atmos. Sci.*, **39**, 643–657, <https://doi.org/10.1007/s00376-021-1289-2>.
- Zhang, R. N., R. H. Zhang, and G. K. Dai, 2022a: Intraseasonal contributions of Arctic sea-ice loss and Pacific decadal oscillation to a century cold event during early 2020/21 winter. *Climate Dyn.*, **58**, 741–758, <https://doi.org/10.1007/s00382-021-05931-5>.
- Zhang, X. D., Y. F. Fu, Z. Han, J. E. Overland, A. Rinke, H. Tang, T. Vihma, and M. Y. Wang, 2022b: Extreme cold events from East Asia to North America in winter 2020/21: Comparisons, causes, and future implications. *Adv. Atmos. Sci.*, **39**, 553–565, <https://doi.org/10.1007/s00376-021-1229-1>.
- Zhang, Y. X., D. Si, Y. H. Ding, D. B. Jiang, Q. Q. Li, and G. F. Wang, 2022c: Influence of major stratospheric sudden warming on the unprecedented cold wave in East Asia in January 2021. *Adv. Atmos. Sci.*, **39**, 576–590, <https://doi.org/10.1007/s00376-022-1318-9>.
- Zheng, F., and Coauthors, 2022a: The predictability of ocean environments that contributed to the 2020/21 extreme cold events in China: 2020/21 La Niña and 2020 arctic sea ice loss. *Adv. Atmos. Sci.*, **39**, 658–672, <https://doi.org/10.1007/s00376-021-1130-y>.
- Zheng, F., and Coauthors, 2022b: The 2020/21 Extremely cold winter in china influenced by the synergistic effect of La Niña and warm arctic. *Adv. Atmos. Sci.*, **39**, 546–552, <https://doi.org/10.1007/s00376-021-1033-y>.
- Zheng, F., and Coauthors, 2022c: Can eurasia experience a cold winter under a third-year La Niña in 2022/23? *Adv. Atmos. Sci.*, in press, <https://doi.org/10.1007/s00376-022-2331-8>. <https://doi.org/10.1007/s00376-022-2331-8>.
- Zhong, L. H., L. J. Hua, and D. H. Luo, 2018: Local and external moisture sources for the arctic warming over the barents-kara seas. *J. Climate*, **31**, 1963–1982, <https://doi.org/10.1175/JCLI-D-17-0203.1>.
- Zhou, T. J., and Coauthors, 2022: 2021: A Year of Unprecedented Climate Extremes in Eastern Asia, North America, and Europe. *Adv Atmos Sci*, **39**, 1598–1607, <https://doi.org/10.1007/s00376-022-2063-9>.